

Fundamental Behavior Analysis of Single-Frequency Sine Wave Forced Oscillator Based on Linear Model and Multi-Time Technique

Arum KITIPONGWATANA¹, Poolsak KOSEYAPORN²,
Jeerasuda KOSEYAPORN¹, Pramote WARDKEIN¹

¹Faculty of Engineering, Dept. of Telecommunications Engineering, King Mongkut's Inst. of Technology Ladkrabang, Ladkrabang, Bangkok, 10520 Thailand

²Faculty of Technical Education, Dept. of Teacher Training in Electrical Engineering, King Mongkut's University of Technology North Bangkok, Bangsue, Bangkok, 10800 Thailand

Akami000@gmail.com, Drpoolsak@gmail.com, Jeerasuda@kmitl.com, Pramote@telecom.kmitl.ac.th

Abstract. *In this article, an excited oscillator which is analyzed by using a multi-time linear analytical model is proposed. An obtained closed-form solution can be exploited not only to explain phenomena in the beat and locked states that are mostly studied in literature but also in an additional state called the non-locked state. With the proposed analysis, it is found that the non-locked state of the oscillator behaves similarly to the up-conversion process. It provides a new point-of-view to the phase noise oscillator. Moreover, our principle indicates that the important factor defining the behavior in each state and state transition is the transfer function of the system. The proposed mathematical model is verified by the experimental and numerical results.*

Keywords

Forced oscillators, non-locked state, beat state, locked state, locked range.

1. Introduction

Nowadays, an electronic circuit [1], [2] which has small size and low-power consuming is in high demand due to an increasing in commercial competition. For this reason, a circuit combining many functions of different electronic circuits is extensively developed. For example, based on the behavior of an oscillator circuit that is forced by an input signal, FM-to-AM conversion circuit [3], FSK-to-ASK conversion circuit [4], demodulating circuit [5], [6], or frequency divider circuit [7] could be possibly made. Nonetheless, bringing forced oscillator into the broader applications, more study of circuit behavior should be further investigated.

From previous works [8-11], it is found that there are two states considered as fundamental phenomena of the excited oscillator, namely, the beat state and the locked

state. The beat state exists when the input frequency is close to a locked range, the system's output signal behaves like a frequency modulation but contains an unsymmetrical-sideband in frequency-domain. The unsymmetrical-sideband has a deviation frequency equal to a frequency difference between the input frequency and the free-running frequency, called the beat frequency. In the past, various of the mathematical models [12-16] was proposed, these models illustrate that the unsymmetrical sideband will be shifted towards the free-running frequency when the input frequency is moved closely to a locked range. However, in these studies have not been stated how much the amplitude of each component should be. The mathematical model proposed in this article will provide the clarification in this issue.

Another state is the locked state in which the output signal of the system synchronizes with the input signal. In the other word, the output frequency is equal to the input frequency. The output amplitude is constant and the output phase is shifted compared to the input signal. With these characteristics of the system in this state, the system is thus applied for a FM-to-AM conversion circuit [3], FSK-to-ASK conversion circuit [4], demodulating circuit [5], [6], or frequency divider circuit [7]. In general, the objective of the analysis in this state is the finding of an accuracy locked condition or a locked-range equation, which they are associated. In the study of [8], [9], [17], [18], the graph of the locked ranges is the symmetrical V shape where the x-axis and the y-axis are amplitude and frequency of the input signal, respectively. The symmetrical V shape is a linear relationship between these variables which is derived only from the elements of the feedback circuit. However, based on the studying in this paper, the locked-range shape is not symmetrical due to the non-linear relationship between both variables which derives not only from the elements of the amplifier but also from the elements of the feedback circuit. Additionally, it is found that the amplitude and phase of output signal will change if the input frequency changes. This phenomenon is applied for FM-to-

AM circuits [3] and FSK-to-ASK conversion circuit [4] but the explanation about this phenomenon is not given in these researches. But with our proposed model, this phenomenon can be clearly explained.

In practical, rather than those two states previously described, there is another state of the excited oscillation system that has never been discussed in the literature. It is the multiplication phenomenon between the free-running signal and the forced response signal. This state appears when the input frequency is far from the free-running frequency. In case of the frequency of the input signal is much less than that of the free-running signal, the system will behave similar to the up-conversion process [19] of a low-frequency noise signal in an oscillator. The behavior in this state will be discussed in this article.

Recently, K. Prompak et al. [20] studied the phenomena of an external excited system in physics application and proposed a mathematical model to explain such phenomena. The model was based on the principle of fundamental system analysis, system transfer function and independence of parameters. From the inspired features of the model in [20], the concept is extended to electrical oscillation system to explain the behavior of the system.

Organization in this paper begins with the idea and mathematical analysis proposed in [20] which is given in Section 2. In Section 3, this model is later applied to analyze and explain the behavior of an oscillator circuit that is stimulated by an external signal. Section 4 illustrates the results in three states of the system obtained from the simulation and experiment. Finally, conclusions of this article are drawn in Section 5.

2. Analysis of Linear System Based on the Technique of [20]

From the idea of research proposed in [20] which is a principle of multi-time technique, a system can be considered by two relative parameters. These parameters are t , which is an inherent time parameter of a natural response of a system ($y_n(t)$), and τ , which is another time parameter of a forced response ($y_f(\tau)$). Since an external signal is fed into the system after the system starts oscillation by amount of time, e.g. Δt , hence, let the relationship between these parameters be $\tau = t + \Delta t$. Based on this consideration, a complete response of the system is

$$y(t, \tau) = y_n(t) + y_f(\tau) \tag{1}$$

and the differential equation of the system is

$$a_2 y''(t, \tau) + a_1 y'(t, \tau) + a_0 y(t, \tau) = b_2 x''(\tau) + b_1 x'(\tau) + b_0 x(\tau) \tag{2}$$

where a_i, b_i are coefficients of the system and $x(\tau)$ is

an external signal. When the system is oscillated, the output signal can be written as

$$y_n(t) = A e^{-\alpha t} \cos(\omega_d t) \tag{3}$$

where $\alpha = \frac{1}{2} \frac{a_1}{a_2}$, $\omega_d = \sqrt{\frac{a_0}{a_2} - \left(\frac{a_1}{2a_2}\right)^2}$ and A is a real constant. For the forced response, it can be determined by

$$a_2 y_f''(\tau) + a_1 y_f'(\tau) + a_0 y_f(\tau) = b_2 x''(\tau) + b_1 x'(\tau) + b_0 x(\tau) \tag{4}$$

where a form of the solution $y_f(\tau)$ is dependent on $x(\tau)$.

The complete solution can be rewritten as

$$y(t, \tau) = K [Y_0 - y_f(\tau)] e^{-\alpha t} \cos(\omega_d t) + y_f(\tau) \tag{5}$$

where

$$K = \frac{1}{e^{-\alpha t_0} \cos(\omega_d t_0)}, y(t = t_0, \tau) = Y_0 \text{ and } \frac{dy(t = t_0, \tau)}{dt} = 0.$$

From (5), it is apparent that the amplitude of the first term is not a constant but it is a summing of a constant and the forced response. This result is different from the complete solution derived by the conventional analysis [21], [22].

3. Phenomena of an Oscillator Excited by an Input Signal

In this section, three states of fundamental behavior of an oscillator that is excited by an input signal are studied. Let the exciting signal be a sine wave which is

$$x(\tau) = X_f \cos(\omega_f \tau) \tag{6}$$

where X_f and ω_f are amplitude and frequency of the external input. From (6), both X_f and ω_f are parameters that can be varied. However, in order to clearly understand the influence of both parameters to the system, firstly, X_f is set to be a small, fixed constant and later its influence will be considered. Therefore, behavior of the system, especially during state changing from non-locked state to beat state and to the locked state is studied through the parameter ω_f . The closed-form solution obtained by using an analysis technique of [20] is considered by changing ω_f from value that is much less than until equal to the free-running frequency (ω_d).

3.1 Analysis of an Oscillator based on Multi-Time Technique

To study behavior of an electrical oscillation system, a second order system consisted of an amplifier and a feedback network as shown in Fig. 1 is employed. From analytical technique of [20], the second order differential

equation when the system is excited by an external signal thus is

$$y''(t, \tau) + 2\xi_s \omega_n y'(t, \tau) + \omega_n^2 y(t, \tau) = b_2 x''(\tau) + b_1 x'(\tau) + b_0 x(\tau) \quad (7)$$

where $y(t, \tau)$ is an output signal which is composed of a natural response ($y_n(t)$) and a forced response ($y_f(\tau)$), $x(\tau)$ is the forcing function given in (6), ω_n is natural frequency, b_2, b_1, b_0 are the system's coefficients, and ξ_s is damping factor of the system. As given in (7), it is seen that all the coefficients in (7) are derived by considering not only from the amplifier but also the feedback network.

Since the system is demanded to generate a constant-amplitude signal by itself, the damping factor has to be a very small value. From (7), the natural response ($y_n(t)$) in oscillation state can be written as

$$y_n(t) = Y_{Sat} \cos(\omega_d t) \quad (8)$$

where Y_{Sat} represents saturated voltage of an amplifier and $\omega_d = \omega_n \sqrt{1 - \xi_s^2}$ represents free-running frequency. If the system is not perturbed, this signal is therefore the output signal generated by the oscillator in a normal state.

For a forced response $y_f(\tau)$ which is related to the external signal, it can be derived by

$$y_f''(\tau) + 2\xi_s \omega_n y_f'(\tau) + \omega_n^2 y_f(\tau) = b_2 x''(\tau) + b_1 x'(\tau) + b_0 x(\tau). \quad (9)$$

By given $\omega_f \ll \omega_n$, the forced response resulted by $x(\tau)$ thus is

$$y_f(\tau) = X_f |H(\omega_f)| \cos(\omega_f \tau + \angle H(\omega_f)). \quad (10)$$

From (10), the important parameters are

$$|H(\omega_f)| = \left[\frac{(b_0 - b_2 \omega_f^2)^2 + (b_1 \omega_f)^2}{(\omega_n^2 - \omega_f^2)^2 + (2\xi_s \omega_n \omega_f)^2} \right]^{1/2} \quad (11)$$

which is the magnitude response of the oscillator. By considering typical oscillators such as Wien-bridge, Twin-T or Colpitts circuits, their normalized magnitude responses as shown in Fig. 2 are similar to that of a low-Q low-pass filter. It implies that any signal will be eliminated if it is outside the pass-band of the system,

$$\angle H(\omega_f) = \tan^{-1} \left(\frac{b_1 \omega_f}{b_0 - b_2 \omega_f^2} \right) \quad (12)$$

which is the phase response. In Fig. 3, the phase response of Wien-bridge, Twin-T and Colpitts circuits are depicted.

As can be seen, the graph of Wien-bridge circuit is inverse compared to those of Twin-T and Colpitts circuits. But when the feedback network is included in consideration, phase of the oscillated signal will be 360 degrees which achieves the Barkhausen's condition.

From the idea given in [20], the complete solution thus can be written as

$$y(t, \tau) = [Y_{Sat} - X_f |H(\omega_f)| \cos(\omega_f \tau + \angle H(\omega_f))] \cos(\omega_d t) + X_f |H(\omega_f)| \cos(\omega_f \tau + \angle H(\omega_f)) \quad (13)$$

which is seen that the amplitude of the natural term changes according to the forced response. Although this equation covers all the coefficients derived from necessary elements of the amplifier and the feedback network, it is not complicated since these coefficients are collected in a form of the transfer function. The obtained transfer function will be an important factor employed to identify each state of the system. The equation given in (13) will be used to describe behavior of the circuit when both frequency (ω_f) and amplitude of the input signal is varied.

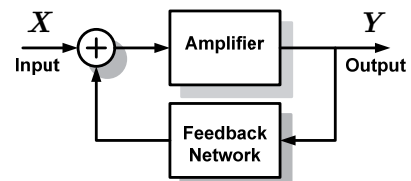


Fig. 1. Model of an oscillator based on a feedback structure.

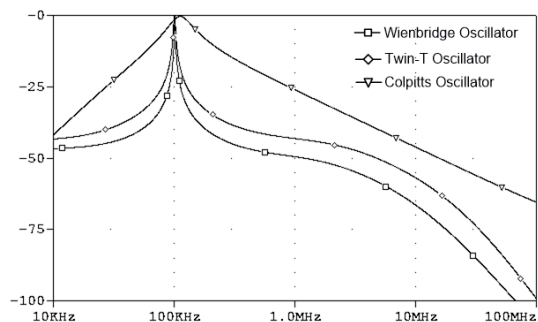


Fig. 2. Normalized magnitude response $|H(\omega_f)|$ of Wien-bridge, Twin-T and Colpitts circuits.

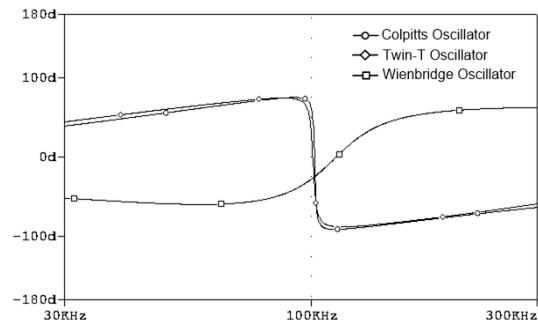


Fig. 3. Phase response $\angle H(\omega_f)$ of Wien-bridge, Twin-T and Colpitts circuits.

3.2 Non-Locked State

This state is the state in which the oscillator is not synchronized with the external signal. The different frequency between the input frequency and the free-running frequency is much larger. In the other word, the input signal does not achieve the locked condition of the system. From (13), Δt in the relationship of $\tau = t + \Delta t$ is assumed to be zero [20], it thus yields

$$y(t) = Y_{Sat} \cos(\omega_d t) - X_f \left| \frac{H(\omega_d - \omega_f)}{2} \right| \cos \left(\left(\omega_d - \omega_f \right) t - \angle H(\omega_d - \omega_f) \right) - X_f \left| \frac{H(\omega_d + \omega_f)}{2} \right| \cos \left(\left(\omega_d + \omega_f \right) t - \angle H(\omega_d + \omega_f) \right) + X_f |H(\omega_f)| \cos(\omega_f t + \angle H(\omega_f)). \tag{14}$$

As shown in (14), $y(t)$ is a combination of four signals with different frequency, which are free-running frequency ω_d (inherent frequency of the system), external-signal frequency ω_f , modulating frequency $\omega_d - \omega_f$, and modulating frequency $\omega_d + \omega_f$. Moreover, it is found that the amplitude of each term depends on the transfer function of the system, except that of the free-running frequency term.

The non-locked state can be divided into 2 cases. The first case is when $\omega_f \ll \omega_d$ as shown in Fig. 4. In this case, frequency components are similar to those of an AM signal whose carrier frequency is ω_d , information frequency is ω_f , and side-band frequencies are $\omega_d - \omega_f$ and $\omega_d + \omega_f$. Since the ω_f term is a part of the output signal, this output signal then cannot be directly used as the AM signal. However, the system output is fed back through a band-pass filter (see Fig. 1) which can eliminate the ω_f term. Then, a pure AM signal can be obtained from the output of the feedback network. In addition, if an input signal is a noise signal, (13) shows that the noise signal will simultaneously disturb amplitude (Y_{Sat}) of the free-running signal which is directly

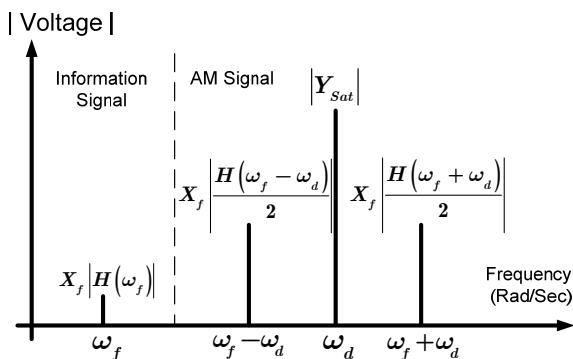


Fig. 4. The non-locked state when $\omega_f \ll \omega_d$.

addition as shown in the second term. The noise disturbance to the amplitude of the free-running signal corresponds to the up-conversion which is disturbing process generally found in oscillators [19]. This disturbance results

in the unwanted sidebands as given by the second and the third terms in (14).

For the second case, it is when $\omega_f \gg \omega_d$ as shown in Fig. 5. In practical, the $\omega_d + \omega_f$ term may not be appeared because it will be eliminated by characteristic of amplitude response ($H(\omega_d + \omega_f)$) of the system and frequency response of active devices (such as a slew rate in op-amp [23]). Similarly for the $\omega_d - \omega_f$ term, it will not be appeared because it is eliminated by amplitude response ($H(\omega_d - \omega_f)$) of the system.

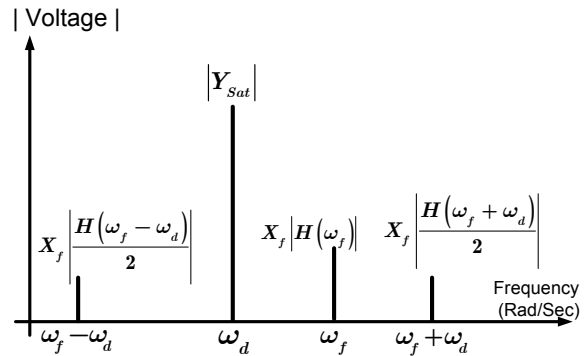


Fig. 5. The non-locked state when $\omega_f \gg \omega_d$.

3.3 Beat State

In previous subsection, before the system changes from the non-locked state to the beat state, the system demonstrates two interesting phenomena when the amplitude of the input signal is fixed and the input signal frequency (ω_f) moves to the free-running frequency (ω_d) where (14) and the $\omega_f \ll \omega_d$ case are considered.

First phenomenon is that values of $X_f |H(\omega_d + \omega_f) / 2|$ and of $X_f |H(\omega_d - \omega_f) / 2|$ will decrease and eventually are significantly less than other terms, then both terms can be neglected. The other phenomenon is that value of $|H(\omega_f)|$ is a constant at the beginning and gradually increases according to a frequency response. Both phenomena are depicted in Fig. 6. In case of $\omega_f \gg \omega_d$, the phenomenon of $|H(\omega_f)|$ is similar to that of the $\omega_f \ll \omega_d$ case but for $X_f |H(\omega_d + \omega_f) / 2|$ and $X_f |H(\omega_d - \omega_f) / 2|$, they will not be appeared according to the transfer functions as described in the previous subsection. Therefore, the output of the system is given as the following.

$$y(t) = Y_{Sat} \cos(\omega_d t) + X_f |H(\omega_f)| \cos(\omega_f t + \angle H(\omega_f)) \tag{15}$$

In (15), it expresses an equivalent equation which is familiar in physics, beat phenomena [24]. But for electronic oscillation circuits, it provides different behaviors [12-16]. By considering the case $\omega_f < \omega_d$, using a relation of Carte-

sian coordinate [19], and letting $\Delta\omega$ be a beat frequency which is the difference between the free-running frequency and the external signal frequency ($\Delta\omega = \omega_d - \omega_f$), (15) is rewritten as

$$y(t) = Y_{Sat} \cos(\omega_f t + \theta(t)) \quad (16)$$

where

$$\theta(t) = \Delta\omega t - \tan^{-1} \left[\frac{k \sin(\Delta\omega t - \angle H(\omega_f))}{1 + k \cos(\Delta\omega t - \angle H(\omega_f))} \right] \quad (17)$$

and

$$k = \frac{X_f}{Y_{Sat}} |H(\omega_f)|. \quad (18)$$

Simultaneously, it is assumed that $Y_{Sat} \gg X_f |H(\omega_f)|$, amplitude of the signal shown in (16) is approximated as

$$Y_{Sat} \approx \left[\frac{Y_{Sat}^2 + X_f^2 |H(\omega_f)|^2}{+2Y_{Sat} X_f |H(\omega_f)| \left[\cos(\Delta\omega t - \angle H(\omega_f)) \right]} \right]^{1/2}. \quad (18)$$

From (18), it is found that k varies linearly with a ratio of X_f / Y_{Sat} whereas k depends on nonlinearly characteristic of $|H(\omega_f)|$. Moreover, it is found that in the locked condition (described in the next subsection), the circuit will not be in the locked state if $|k| < 1$.

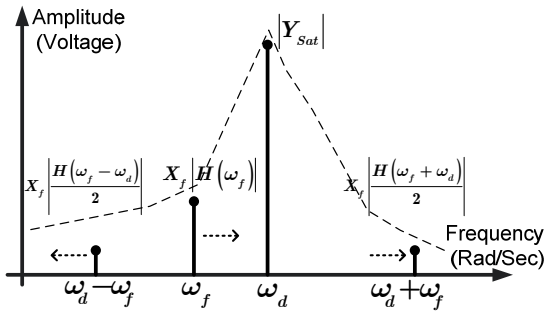


Fig. 6. Phenomenon of the circuit when ω_f moving into beat state.

When the system is in this state, $\theta(t)$ will be a periodic function whose frequency is $\Delta\omega$. It causes $y(t)$ to behave as a FM signal, whose an instantaneous frequency of $y(t)$ in this state is

$$\frac{d}{dt}(\omega_f t + \theta(t)) = \omega_d + \Delta\omega \sum_{n=1}^{\infty} (-1)^n k^n \cos(n(\Delta\omega t - \angle H(\omega_f))). \quad (19)$$

This equation points out that the output frequency deviates periodically from the free-running frequency and the

deviation strength depends on k . By solving (19), the output signal equation in this state thus is

$$y(t) = Y_{Sat} \cos \left(\omega_d t + \sum_{n=1}^{\infty} (-1)^n \frac{k^n}{n} \sin \left(n(\Delta\omega t - \angle H(\omega_f)) \right) \right). \quad (20)$$

In order to gain insight into the behavior in this state, the frequency components of the output signal will be determined. In case that the input frequency (ω_f) is above the non-locked state range and a locked condition cannot be achieved, the frequency difference is $\Delta\omega_f$. In this situation, k shown in (20) is a small value and also for k^2, k^3, \dots which can be neglected. Hence, the spectrum of the output signal in this situation is

$$y(t) = Y_{Sat} \cos(\omega_d t) + Y_{Sat} \frac{k}{2} \sin(\omega_f t + \angle H(\omega_f)) - Y_{Sat} \frac{k}{2} \sin((\omega_d + \Delta\omega_f)t - \angle H(\omega_f)). \quad (21)$$

From (21), it is found that the sidebands at ω_f and $\omega_d + \Delta\omega_f$ depend on k and have equal magnitude. If the input frequency (ω_f) is moved closely to the free-running frequency, it causes amplitude of k and k^2 shown in (20) dominant. By using the power series approximation, the components of the output signal will be

$$y(t) = Y_{Sat} \left(1 - \frac{k^2}{4} - \frac{k^4}{16} \right) \cos(\omega_d t) + Y_{Sat} \left(\frac{k^3}{8} + \frac{k}{2} \right) \cos(\omega_f t + \angle H(\omega_f)) + Y_{Sat} \left(\frac{k^3}{8} - \frac{k}{2} \right) \cos((\omega_d + \Delta\omega_f)t - \angle H(\omega_f)). \quad (22)$$

This equation shows that amplitude of $\omega_d + \Delta\omega_f$ and ω_d terms decreases whereas amplitude of ω_f term increases, resulting in unsymmetrical sidebands. This behavior indicates that the more the input frequency is close to the free-running frequency, the more power it gets, which is contradictory to the other two terms. This amplitude variation appears until the system moves into the locked state. However, amplitude of each component cannot be exactly determined since an oscillator is always controlled by an amplitude adjusting mechanism which is naturally in the circuit. According to [9], the probability is employed to indicate how much the amplitude of each spectrum should be in this state. It is found that the probability function whose k is a factor given in [9] is identical to the normalization of (22) by the free-running amplitude ($y(t) / Y_{Sat}$).

3.4 Locked State

The locked state is the state in which the output signal is synchronized with the external signal. In the other word, the output frequency is identical to the frequency of the

input signal where the amplitude and phase of the output signal are constants. This behavior is happened when the external signal achieves the locked condition.

When the circuit is shifted to the locked state, it will generate the oscillation signal whose frequency is equal to that of the input frequency. Therefore

$$\frac{d[\omega_d t + \theta(t)]}{dt} = \omega_f,$$

and by using

$$\frac{d}{dt} \tan^{-1}(\phi) = \left[\frac{1}{1 + \phi^2} \right] \frac{d(\phi)}{dt}$$

hence, (17) becomes

$$1 + k \cos(\Delta\omega t - \angle H(\omega_f)) = 0. \tag{23}$$

From $k = \left| \frac{X_f}{Y_{Sat}} H(\omega_f) \right|$ and $|\cos(\phi)| \leq 1$, the circuit condition will move toward to the locked state, if (24) is true.

$$|k| = \left| \frac{X_f H(\omega_f)}{Y_{Sat}} \right| \geq 1. \tag{24}$$

From (24), it is found that the locked condition depends directly on the input-signal amplitude and the transfer function, but depends inversely on the free-running signal amplitude. Note that, k is not only a key factor of the locked condition but it also determines the amplitude of each component in the beat state. From the locked condition, the locked range which is

$$|X_f| \geq |Y_{Sat} / H(\omega_f)| \tag{25}$$

can be shown in Fig. 7 where the x-axis and y-axis are the amplitude and frequency of the input signal, respectively. In Fig. 8, an asymmetrical shape of the graph is resulted from the inversed transfer function which is scaled by the free-running signal amplitude. Asymmetry of this graph will be obviously appeared when the input-signal amplitude is large.

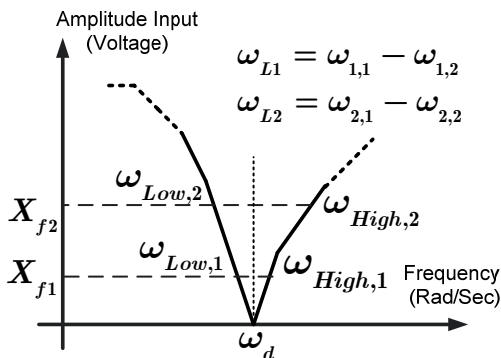


Fig. 7. The unsymmetrical locked range.

For some types of oscillators whose order of the transfer function is greater than two, handout analysis of the transfer function may be impossible. However, the locked condition in (24) can be achieved by using a computer simulation such as SPICE to find the amplitude response due to the input signal. The frequency that has amplitude response equal to the amplitude of the free-running signal (Y_{Sat}) can be employed to determine the locked range of the circuit, as an example shown Fig. 8.

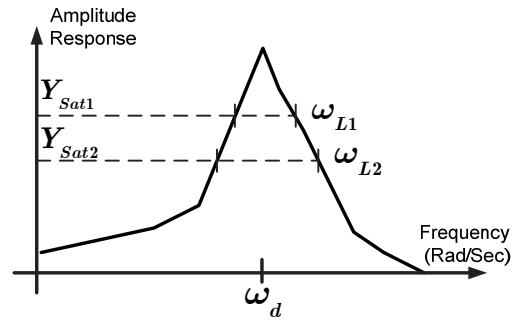


Fig. 8. Finding of the locked range by using amplitude response and voltage saturation.

In addition, after considering (11), it is found that when ω_f gets much closer to ω_n , ξ_s will usually be small in order to maintain an oscillation of system. Consequently, the value of $H(\omega_f)$ will increase rapidly due to $(\omega_n^2 - \omega_f^2)^2$ as shown in the denominator of (11). When the system condition reaches to the locked state, the constraint shown in (24) must be obtained, which is $|k| \gg 1$. The output signal of the circuit at this state can be rewritten as

$$y(t) = X_f |H(\omega_f)| \cos(\omega_f t + \angle H(\omega_f)). \tag{26}$$

This equation shows that the circuit only responses to the influence of the input signal. Therefore, phase and amplitude of the output signal depends on the phase response and magnitude response of the system, respectively. Throughout the analysis, the considered output is the output of the amplifier (see Fig. 1). But in real world application, it is difficult to correctly define the amplitude of the output signal in practical. Since the amplitude is controlled by controlling mechanism related to characteristics of the employed active device, for example, the voltage saturation and the slew-rate of an op-amp [25]. However, amplitude of the output signal is always not greater than the voltage saturation of the circuit. Let us consider the practical output signal whose the amplitude is maximum, hence, (26) is rewritten to be

$$y(t) = Y_{sat} \cos(\omega_f t + \angle H(\omega_f)). \tag{27}$$

It is seen that phase of the output signal depends on frequency of the input signal and the relationship is linear if the input-signal frequency is much closer to the oscillation

frequency (ω_d). With this characteristic, the excited oscillator in the locked state is thus applied to be a demodulating circuit by using the phase difference between the phase of the output signal and the phase of the input signal [6].

From the structure of the system in Fig. 1, the signal in (27) will be fed back through the feedback network which generally is the band-pass circuit, the feedback-network output is then given by

$$y_{BP}(t) = Y_{Sat} \left| H_{BP}(\omega_f) \right| \cos \left(\omega_f t + \angle H(\omega_f) + \angle H_{BP}(\omega_f) \right). \quad (28)$$

This equation shows that not only phase of the output is proportional to frequency of the input signal; amplitude of the output also depends on frequency of the input signal as well. With these features, the circuit can be applied for FM-to-AM conversion circuit [3] and FSK-to-ASK conversion circuit [4].

4. Experimental Results

In this section, the proposed principle is verified by experiment. All three states are confirmed by supplying the input-signal to an oscillator circuits. Moreover, in order to observe the behaviors clearly, both the output and input signals will be shown in time-domain using a low-frequency oscillator constructed by an active device (Op-amp) and RC passive devices.

4.1 Non-Locked State

The Wien-bridge oscillator depicted in Fig. 9 which has a second-order transfer function will be employed to show the behavior in the non-locked state. This circuit is designed to oscillate at 150 kHz ($Q = 0.23m$), where an op-amp is LM351 and the power supply is $\pm 5V$. The input signal is a sinusoidal signal whose amplitude and frequency is 0.1 Vp and 10 kHz, respectively.

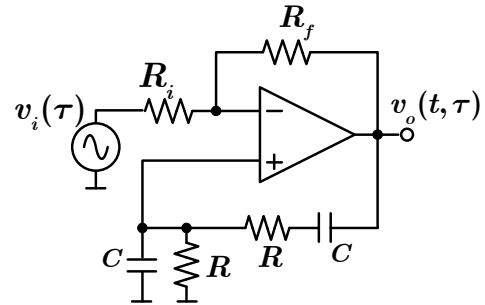


Fig. 9. Structure of Wien-bridge oscillator for testing non-locked state.

When the input signal frequency is moved closely to the free-running signal frequency, there are two interesting behaviors occurred in the circuit. First, the sidebands move away from the free-running signal frequency and their amplitude decreases until fade away. Second, amplitude of the forced response slightly increases. These phenomena are demonstrated in Fig. 10(a-e) whose amplitude of each

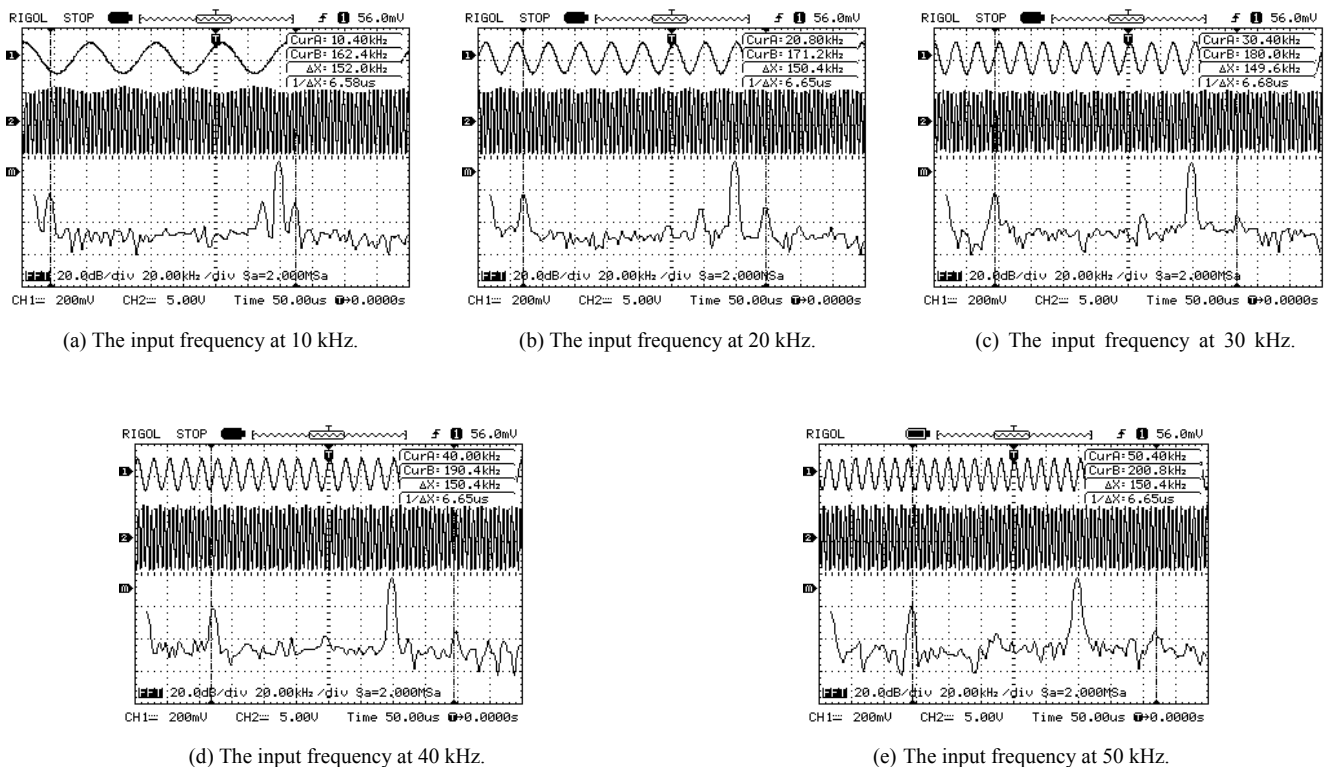


Fig. 10. The experimental results of the Wien-bridge oscillator for $\omega_f \ll \omega_d$ case.

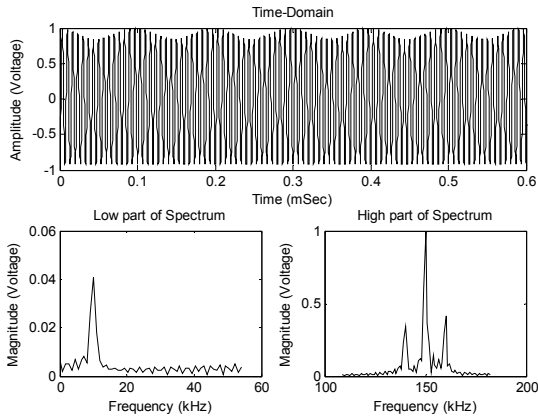


Fig. 11. Numerical results in time domain (top) and frequency components (bottom) are of Wien-bridge’s complete solution obtaining the proposed analysis.

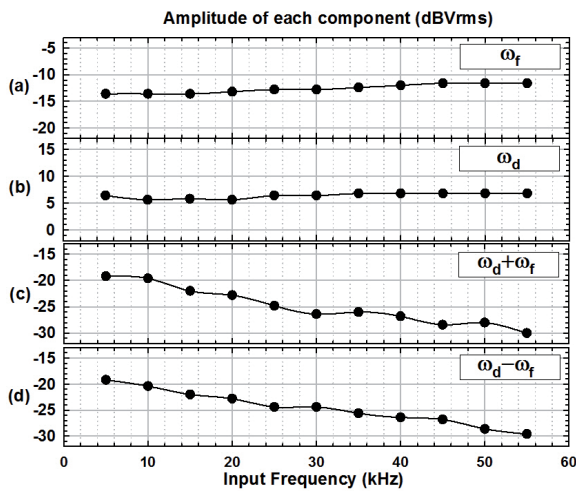


Fig. 12. Amplitude of each term of the output signal in the non-locked state when $\omega_f \ll \omega_d$ where (a), (b), (c) and (d) are amplitude of ω_f , ω_d , $\omega_d + \omega_f$ and $\omega_d - \omega_f$ terms, respectively.

frequency component is drawn in Fig. 12. These phenomena also agree well with the proposed principle given in Section 3.5.

The experimental result is shown in Fig. 10(a) where Ch.1 and Ch.2 demonstrate the output and input signals, respectively. It is found that upper envelope of the output signal is similar to the AM signal, whereas lower envelope is not, due to the last term of (13). Moreover, the spectrum of the output signal can describe the multiplication of the signals shown in the first term of (13). To obtain more clear result, the complete solution, derived by the multi-time analysis technique given in (13), is numerically plotted in Fig. 11 where (A) is the normalized complete response and (B) is the component of normalized complete response. This figure clearly illustrates that the signals in both domains derived from the experimental results in Fig. 10(a) are in accordance with the theoretical analysis as expressed in (13).

In order to clearly illustrate the multiplying phenomenon in this state, a non-single tone signal is fed into the

circuit. Fig. 13 shows the experimental result where the input signal (Ch.1) is a square wave signal with 15 kHz and 0.1 Vp. As can be seen, upper envelope of the output signal (Ch. 2) is similar to the input signal. This results from the multiplication of the free-running term and the external response term. In the frequency domain (Ch. m), the spectrum is divided into two parts where the low-frequency part is of the external response and the other part consists of the free-running frequency and sidebands which is up converted from the low-frequency part.

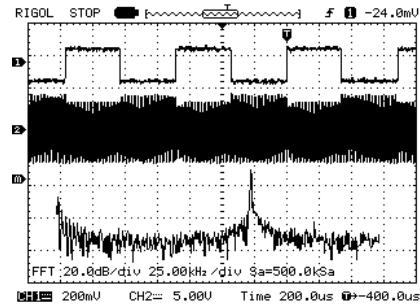
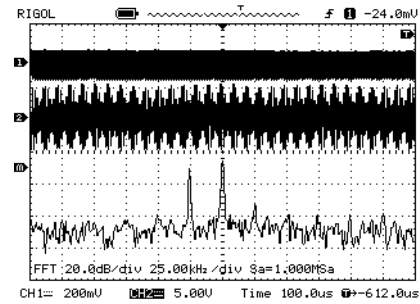


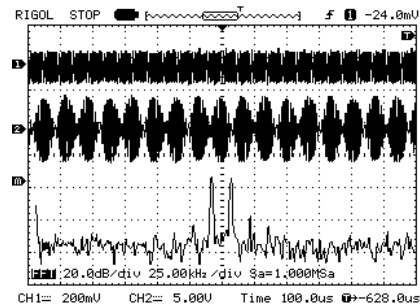
Fig. 13. Experimental result in the non-locked state when the input signal is a non-single tone signal (the square wave signal).

4.2 Beat State

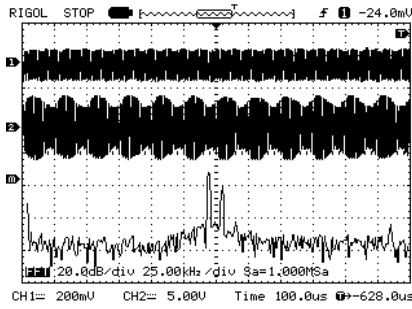
In this state, the Wien-bridge oscillator which is employed in experiment of the non-locked state will be continuously used. The sinusoidal input signal is set to the frequency above 55 kHz which is in a range that the $\omega_d + \omega_f$ and $\omega_d - \omega_f$ terms are faded away. When the input signal frequency is close to the locked range, the system will fall into the beat state. Fig. 14(a) is the experimental result in this state where Ch.1 is the sinusoidal input signal



(a) The input frequency at 125 kHz.



(b) The input frequency at 133 kHz.



(c) The input frequency at 137 kHz.

Fig. 14. Experimental results in the beat state of the system.

with 125 kHz and 0.1 V_p and Ch.2 is the output signal whose envelope varies slowly. This envelope is resulted from a narrow deviation of the free-running signal frequency which equals to the beat frequency. The spectrum of the output signal (Ch. m) is similar to that of a narrow-band FM signal but are not symmetrical. Additionally, a distance between each spectrum is 25 kHz. In Fig. 14(a-c), the experimental results are obtained when the input signal frequency is increased. It is found that amplitude of the ω_f term increases and amplitude of the ω_d term decrease continuously. Moreover, amplitude of $\omega_d + \Delta\omega$ is apparent when the input signal frequency is located at 100 kHz and increases continuously. When the input-signal frequency is about 136 kHz, amplitude of both ω_d and $\omega_d + \Delta\omega$ terms decreases gradually. Finally, the system is in the locked state. Amplitude variation of each frequency component is concluded in Fig. 15.

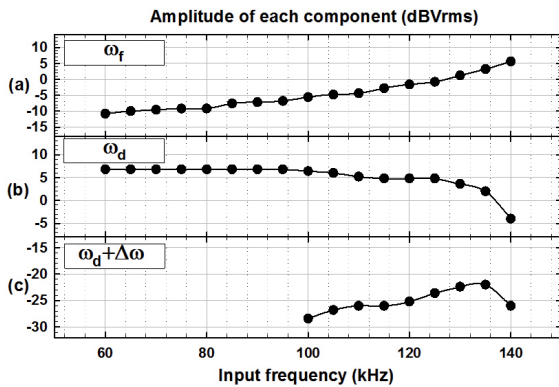
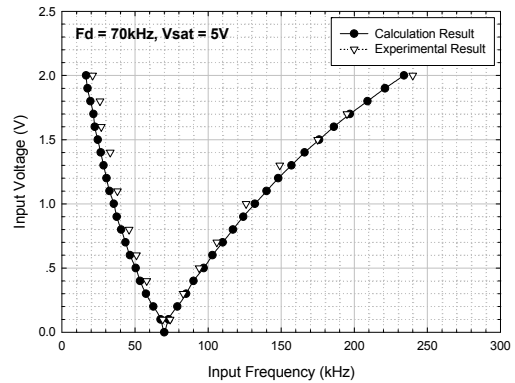


Fig. 15. Amplitude of each frequency component in the beat state where (a), (b) and (c) are amplitude of ω_f , ω_d , and $\omega_d + \Delta\omega$ terms, respectively.

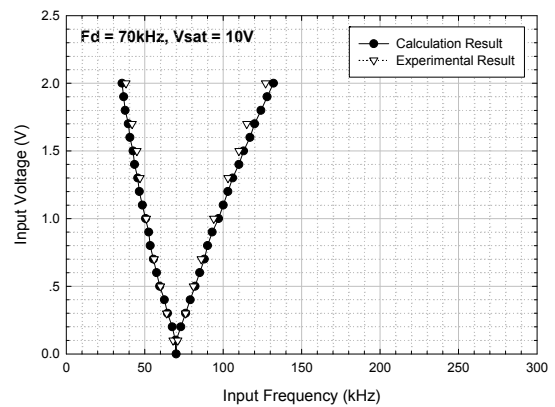
4.3 Locked State

To confirm the locked range obtained from the proposed analysis, the Wien-bridge oscillator is employed in experiment as well. The locked range obtained from experiment and numerical results of using (25) are compared. In the experiment, the designed oscillator is set to maintain frequency at 70 kHz based on LM351 op-amp. To study the impact of amplitude of oscillation and external signals, free-running signal amplitude (V_{Sat}) is selected as 5 V_p, 10 V_p and 15 V_p and the sinusoidal external signal is chosen to be 0.1 V_p to 2 V_p.

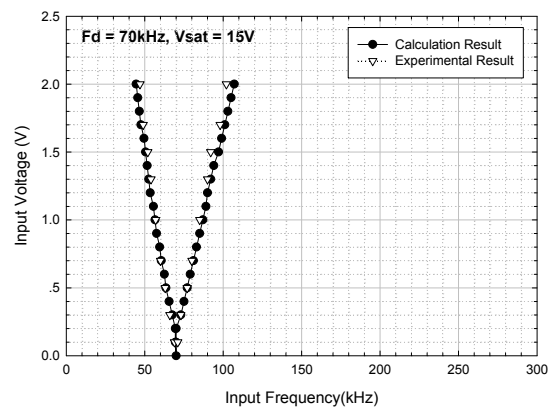
The experimental results are shown in Fig. 16(a) to (c). It is seen that the locked range is directly varied with the input-signal amplitude but depends inversely on the oscillation signal amplitude as explained in (22). In case that the free-running signal amplitude is 5 V_p, the locked range appears unsymmetrical V shape which is resulted from the transfer function. But for the other two cases (Fig. 16(b), (c)), this asymmetrical shape is not apparent. This is because the transfer function is scaled by the large oscillation signal amplitude. Additionally, the results also



(a) The oscillation-signal amplitude at 5 V_p.



(b) The oscillation-signal amplitude at 10 V_p.



(c) The oscillation-signal amplitude at 15 V_p.

Fig. 16. Locked range of the Wien-bridge oscillator (50 kHz), due to the influence of amplitude of the external signal and the free-running signal.

demonstrate that the locked range obtained from the proposed analysis is close to the result obtained from the experiment.

To confirm that frequency, amplitude and phase of the output signal depend on the input-signal frequency, this relationship is confirmed by the computer simulation. The Wien-bridge oscillator whose frequency is 95 kHz and amplitude is 4 Vp is set up. Fig. 17 shows the simulation result of circuit when applying the input signal whose amplitude is 50 mVp. In this figure, Ch.1 is the 95 kHz input signal, Ch.2 is the output signal of the amplifier and Ch.3 is the output signal of the feedback network. It can be seen in this figure that phase shift of the output signals (Ch.2, Ch.3) are obtained from the input signal (Ch.1). It is found that the output signal of the amplifier (Ch.2) is saturated by amplitude adjusting mechanism.

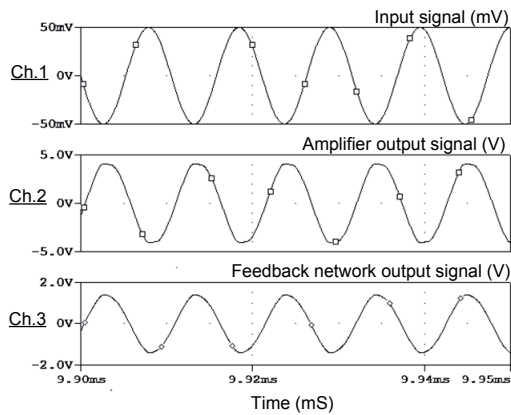


Fig. 17. Simulation result of Wien-bridge oscillator having 95 kHz and 4 Vp by feeding sine wave.

Due to amplitude limiting of the circuit as shown in Fig. 17, it thus makes the consideration of the amplifier’s output signal in time domain difficult. Hence, amplitude variation of the output signal will be only considered at the feedback-network which is shown in Fig 18.

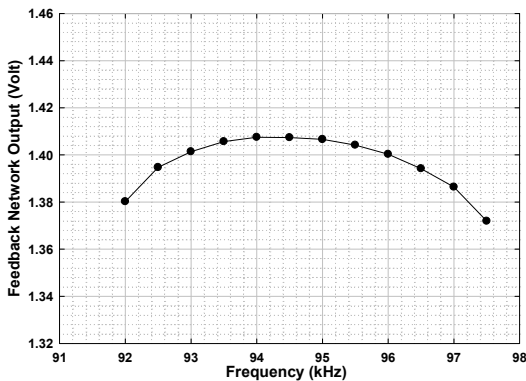


Fig. 18. Simulation result of amplitude variation of the feedback-network output with respect to the input-signal frequency.

The variation of graph shows a curve whose maximum point is at 94.5 kHz. This curve is corresponding to frequency response of the feedback network described in

(24). With this feature in the locked state, the forced oscillator can be applied for FM-to-AM conversion circuit.

From the simulation result as shown in Fig. 19, the phase relation in the locked state is demonstrated where (●) denotes the phase relation of the amplifier output and (○) represents the phase relation of the feedback-network output. It can be seen that phase shift in both output signals are resemble but not identical. The reason is because of the phase shift property of the feedback network. The output of the feedback network will have a very small phase shift when the input-signal frequency is very close to the natural frequency of the feedback circuit, having the structure similar to the band-pass filter or the tuned circuit. With the phase shifting property, the oscillator in the locked state can therefore be applied for the demodulating circuit.

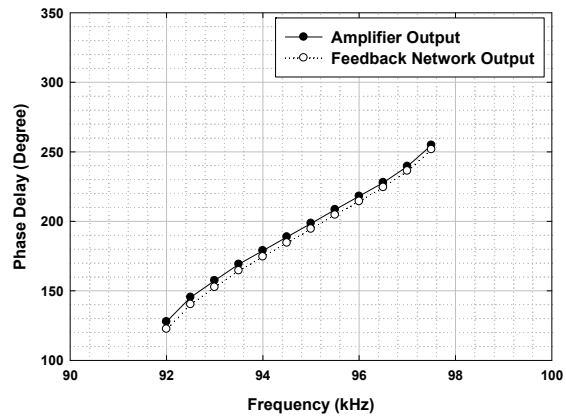


Fig. 19. Phase shifting of the output signal of the amplifier (●) and the feedback network (○) compared at each input-signal frequency.

5. Conclusion

This article proposes the study of fundamental behavior of the oscillation system fed by a single tone signal. This study is based on the multi-time analytical model. The closed form solution obtained by the proposed model can be employed to explain all behaviors in 3 states and also during the state transition.

For the oscillator in the non-locked state, it expresses the multiplication behavior between the free-running signal and the forced response. The product of the multiplication depends on the transfer function of the system. This state occurs when the input frequency is much far from the free-running signal frequency. In case that the input signal frequency is much less than the free-running signal frequency, the output signal will behave like an AM signal added with the forced response of the information signal (if the input signal is considered as an information signal). Therefore, the circuit in this state can be applied for the AM modulator. On the contrary, if the input signal is a low-frequency noise signal, the sidebands of the free-running signal frequency will become a skirt-like spectrum [26]. This behavior is according to the noise up-conversion process. It

implies that the proposed mathematical model provides a new point of view to an issue of disturbance due to the low-frequency noise signal.

When the input frequency is close enough to the locked range, both sidebands will fade away and the system will be in the beat state. The output signal behaves similar to the narrow-band FM signal whose the sidebands are not symmetrical. The solution in this state also can answer the question that how much the probability should be. This probability function depends on the transfer function, the input signal amplitude and the oscillation signal amplitude. When the input signal frequency is in the locked range, overall power of the output signal will overcome that of the forced response signal.

Finally, the locked state, the locked condition or the locked range depends on the input signal amplitude, the free-running signal amplitude and the transfer function, which is a function of the input signal. Because the characteristic of the transfer function is not linear, the locked range thus has unsymmetrical V shape. Moreover, the amplitude and phase of output signal are varied with the input signal frequency. The circuit in this state can be applied for the FM-to-PM and FM-to-AM convertor.

Acknowledgement

Financial support from the Thailand Research Fund through the Royal Golden Jubilee Ph.D. Program (Grant No. PHD/0014/2553) to Arum Kitipongwatana and Paramote Wardkein are acknowledged.

References

- [1] KHATEB, F., BAY ABO DABBOUS, S., VLASSIS, S. A survey of non-conventional techniques for low-voltage low-power analog circuit design. *Radioengineering*, 2013, vol. 22, no. 2, p. 415 to 427.
- [2] SZENDIUCH, I. Development in electronic packaging moving to 3D system configuration. *Radioengineering*, 2011, vol. 20, no. 1, p. 214 - 220.
- [3] BISWAS, B. N., CHATTERJEE, S., PAI, S. New observations on bias current variation of op amp oscillators. In *Proceedings of General Assembly and Scientific Symposium*, 2011, p. 1- 4.
- [4] BAE, J., YAN, L., YOO, H. A low energy injection-locked FSK transceiver with frequency-to-amplitude conversion for body sensor applications. *IEEE Journal of Solid-State Circuits*, 2001, vol. 46, p. 928 – 938.
- [5] YAN, H., MACIAS-MONTERO, J. G., AKHNOUKH, A., DE VREEDE, C. N. L., LONG, R. J., BURGHARTZ, N. J. An ultra-low-power BPSK receiver and demodulator based on injection-locked oscillators. *IEEE Transactions on Microwave Theory and Techniques*, 2011, vol. 59, p. 1339 – 1349.
- [6] WANG, C. S., CHU, K. D., WANG, C. K. A 0.13 CMOS 2.5Gb/s FSK demodulator using injection-locked technique. In *Proceeding of IEEE Radio Frequency Integrated Circuits Symposium*, 2009, p. 563 – 566.
- [7] RATEGH, H. R., LEE, T. H. Superharmonic injection-locked frequency dividers. *IEEE Journal of Solid-State Circuits*, 1999, vol. 34, no. 6, p. 813 – 822.
- [8] ADLER, R. A study of locking phenomena in oscillators. *Proceedings of the IEEE*, 1973, vol. 61, no. 10, p. 1380 – 1386.
- [9] RAZAVI, B. A study of injection locking and pulling in oscillators. *IEEE Journal of Solid-State Circuits*, 2004, vol. 39, no. 9, p. 1415 – 1425.
- [10] PACIOREK, L. J. Injection locking of oscillators. *Proceeding of the IEEE*, 1965, vol. 53, no. 11, p. 1723–1727.
- [11] KUROKAWA, K. Injection locking of microwave solid-state oscillators. *Proceeding of the IEEE*, 1973, vol. 61, no. 10, p. 1336 to 1410.
- [12] STOVER, H. L. Theoretical explanation for the output spectra of unlocked driven oscillators. *Proceeding of the IEEE*, 1996, vol. 54, p. 310 – 312.
- [13] DEKLEVA, J., ZANCHI, I. Improved calculation for the output spectra of unlocked driven oscillator. *Proceedings of the IEEE*, 1972, vol. 60, p. 135 – 136.
- [14] XIAOLUE, L., ROYCHOWDHURY, J. Capturing oscillator injection locking via nonlinear phase-domain macromodels. *IEEE Transactions on Microwave Theory and Techniques*, 2004, vol. 52, p. 2251 – 2261.
- [15] ARMAND, M. On the output spectrum of unlocked driven oscillators. *Proceeding of the IEEE*, 1969, vol. 57, p. 789 – 799.
- [16] MAFFEZZONI, P., D'AMORE, D. Evaluating pulling effects in oscillators. *IEEE Transaction on Computer-Aided Design of Integrated Circuits and Systems*, 2009, vol. 28, no. 1, p. 22 – 31.
- [17] MAFFEZZONI, P. Analysis of oscillator injection locking through phase-domain impulse-response. *IEEE Transactions on Circuits and Systems I: Fundamental Theory and Applications*, 2008, vol. 55, p. 1297-1305.
- [18] MAFFEZZONI, P., D'AMORE, D., DANESHGEAR, S., KENNEDY, M. P. Analysis and design of injection-locked frequency dividers by means of a phase-domain macromodel. *IEEE Transaction Circuits and Systems*, 2010, vol. 57, no. 11, p. 2956 –2967.
- [19] RUBIOLA, E. *Phase Noise and Frequency Stability in Oscillators*. Cambridge Univ. Press, 2009.
- [20] PROMPAK, K., KAEWPOOSUK, A., MANEECHUKATE, T., MANEEJIRAPRAKARN, N., PENGPAD, S., WARDKEIN, P. A new oscillation frequency discovery of the driven spring-mass system predicted by the multi-time differential equation. *European Journal of Scientific Research*, 2012, vol. 92, no. 3, p. 397–410.
- [21] LATHI, B. P. *Signal Processing and Linear System*. Berkeley-Cambridge, 1998.
- [22] THOMSON, W. T. *Theory of Vibration with Applications*. Prentice-Hall of India Private Limited, New Delhi, 1975.
- [23] FRANCO, S. *Design with Operational Amplifiers and Analog Integrated Circuits*. McGraw-Hill, 2002.
- [24] JEWETT, J. W., SERWAY, R. A. *Physics for Scientists and Engineers with Modern Physics*. Thomson, 2008
- [25] HUERTAS, J. L., BELEN, P. V., ANGEL R. V. Analysis and design of self-limiting single-op-amp RC oscillators. *International Journal of Circuit Theory and Applications*, 1990, vol. 18, p. 53 to 69.
- [26] RAZAVI, B. *RF Microelectronics*. Prentice-Hall, 1997.

About Authors ...

Arum KITIPONGWATANA received B.Sc. degree in Electrical Engineering from King Mongkut's University of Technology North Bangkok (KMUTNB), and M.Eng degree in Electrical Engineering from Mahanakorn University, Bangkok, Thailand, in 2007 and 2009, respectively. Now he is studying in D. Eng. degree in Electrical Engineering at King Mongkut's Institute of Technology Ladkrabang (KMITL), Thailand.

Jeerasuda KOSEYAPORN graduated M.S. and Ph.D. degrees in Electrical Engineering from Vanderbilt University, Nashville, TN, USA, in 1999 and 2003, respectively. She is currently an associate professor of Telecommunica-

tion Engineering Department, Faculty of Engineering, KMITL, Thailand.

Poolsak KOSEYAPORN graduated M.S. and Ph.D. degrees in Electrical Engineering from Vanderbilt University, Nashville, TN, USA, in 1999 and 2003, respectively. He is currently an assistant professor at the Dept. of Teacher Training in Electrical Engineering, KMITNB.

Paramote WARDKEIN received his M.E. and D.Eng. degree in Electrical Engineering from King Mongkut's Institute of Technology Ladkrabang (KMITL), Bangkok, Thailand, in 1990 and 1997, respectively. He is now an associate professor of the Dept. of Telecommunication Engineering, Faculty of Engineering, KMITL, Thailand.